

LIFE-TIME PREDICTION FOR ANCHORAGE SYSTEMS

I. BOUMAKIS*, J. VOREL*, M. MARCON*, AND R. WENDNER*

*University of Natural Resources and Life Sciences
Christian Doppler Laboratory for Life-Cycle Robustness in Fastening Technology
Vienna, Austria
e-mail: ioannis.boumakis@boku.ac.at
jan.vorel@boku.ac.at
marco.marcon@boku.ac.at
roman.wendner@boku.ac.at

Key words: Cohesive Fracture, Fiber Reinforced Concrete, Composites, Durability

Abstract. The life-time prediction of fastening systems under sustained loads requires, among others, a suitable numerical solution strategy and viscoelastic constitutive models that can reproduce well the material specific characteristics. The formulation and calibration of viscoelastic models can be based on a topdown approach from observed macroscopic response or, alternatively, a bottom-up approach can be pursued. In the simplest case a fine scale model can represent the system response of bonded and mechanical anchors with contributions of each component, namely (i) concrete, (ii) steel, and (iii) mortar, and the respective interfaces, which are calibrated individually based on quasi-static tests and creep tests. Further homogenization steps allow the derivation of each materials creep response from their respective sources at lower scales hydrates for concrete and the polymer matrix. In this contribution we will analyze and decompose the creep deformations of two typical bonded anchor systems. The visco-elastic behavior of concrete, modeled according to the micro-prestress solidification theory, and of the polymer mortars, represented by a Kelvin-Chain, will be calibrated based on macroscopic creep tests of suitable size. The bond-law for the top-down approach of bonded anchors, which represents the smeared response of interfaces and mortar layer, will be calibrated on suitable pull-out tests. Sustained load tests on all three types of fastening systems serve for the validation, and if necessary, for the detection of neglected mechanisms.

1 INTRODUCTION

Fastening technology plays a key role in structural engineering. Particularly, there is always the necessity of connecting different structural elements, assemblage of precast elements, and the attachment of non-loading bearing components. The previous can be done during construction, as well as during strengthening and retrofitting. The importance of fastenings systems in structural engineering is amplified by the amount of damage an entire system might suffer due to the failure of few comparably cheap fastening elements. For instance, the

Big Dig ceiling collapse, on July 10, 2006, was caused by the failure of different anchor elements and lead to casualties as well as economic damage tremendously larger than the value of the products themselves. Therefore, a more accurate forecast of the long term behavior of fastenings systems is an essential part of their safe design.

For a complete insight into the long term behavior of fastening systems, an understanding of the critical damage mechanisms is required, that lead to deterioration of the involved materials – concrete, steel, and adhesives – in course

of time. Such phenomena may be, among others, creep of concrete and mortars, shrinkage of concrete, partly balanced by the aging of concrete and adhesive. Concerning the creep mechanism, a framework that couples the physical and chemical phenomena, that occur in concrete during hydration, to a mechanical model including damage, is required. The effect of concrete creep on the long term performance of bonded anchors under sustained load, is quantified numerically in this contribution, using the hygro-thermo-chemical (HTC) model [10, 11], for the simulation of the moisture transport, hydration, and temperature evolution, and the micro-prestress solidification theory (MPS) [2, 3], which relates the output of HTC variables into creep, shrinkage and thermal strains in a rate-type form. The mechanical constitutive model applied in this study is the well known lattice discrete particle model (LDPM) [8, 9].

In order to quantify the effect of concrete creep, a large amount of tests is required. Specifically, for two selected concrete classes C25/30 and C50/60, full experimental characterizations of the material properties are obtained from standard cubes and prisms at various ages between 2 days and 56 days, providing cylinder compressive strength $f_c(t)$, Young's modulus $E_c(t)$, indirect tensile strength through three point bending and Brazilian splitting tests $f_t(t)$, and fracture energy $G_F(t)$ as functions of time. These data are used for the calibration of the mechanical constitutive model. Additionally, the aforementioned model is validated, using data of pull-out tests of bonded anchors at different ages. The elastic-bond law for the system simulations is calibrated and validated using the results of two different configurations of pull-put tests with close and wide support.

On the other hand, internal humidity and temperature evolution is measured in two cubes of 20 cm edge length, so that the HTC parameters can be calibrated. Finally, for the calibration and validation of the MPS type creep and shrinkage model a series of creep and shrinkage tests are used. These include sealed and unsealed specimens, loaded at 3, 7, and 28 days,

DOI 10.21012/FC9.141
as well as the companion specimens of drying shrinkage starting at the same ages, and sealed specimens starting measuring exactly after demolding, roughly 24 hours after casting, for autogenous shrinkage. Since these tests demand extended times of measuring, a first approach is to use data from the Northwestern University database for creep and shrinkage [12] for the preliminary phase of this project. Particularly, data sets of Brooks [7] are used for the case of concrete class C25/30. The dataset selection is driven by its relatively similar compositions, as well as by the available duration of experimental data for both components of creep as well as shrinkage.

2 Formulation

In this investigation the hygro-thermo-chemical model [10, 11], is used, which formulates and solves the problems of moisture transport, hydration and temperature evolution. The strength of the model is indicated by formulating such a complicated task-combining different chemical reactions, and physical mechanisms-using finally just the following two governing equations, with solely temperature and relative humidity as the only state variables

$$\begin{aligned} \nabla \cdot (D_h \nabla h) - \frac{\partial w_e}{\partial h} \frac{\partial h}{\partial t} \dot{\alpha}_c \\ - \frac{\partial w_e}{\partial \alpha_s} \dot{\alpha}_s - \dot{w}_n = 0 \end{aligned} \quad (1)$$

and

$$\begin{aligned} \nabla \cdot (\lambda_t \nabla T) - \rho c_t \frac{\partial T}{\partial t} \\ + \dot{\alpha}_c c \tilde{Q}_c^\infty + \dot{\alpha}_s s \tilde{Q}_s^\infty = 0 \end{aligned} \quad (2)$$

where D_h permeability, w_e evaporable water, α_c and α_s hydration and silica fume reaction degrees respectively, w_n non-evaporable water, ρ concrete density c_t isobaric heat capacity, λ_t heat conductivity, c and s , cement and silica fume content, \tilde{Q}_c^∞ and \tilde{Q}_s^∞ cement hydration and silica fume reaction enthalpies, respectively. The multi-physics problem is formulated

and solved in the framework of continuum elements while the mechanical problem is set up as a discrete model in an explicit framework.

The creep problem is solved using the MPS theory, which splits the total strain in different strain components, using the principle of superposition. As it is shown in Figure 1, a rheological model can be adopted to link the different strain contributions to different components.

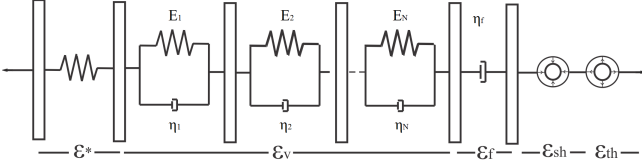


Figure 1: Rheological model of MPS theory

In that approach, the elastic response ϵ^* is described by a spring, the viscoelastic response, linked to short term creep, ϵ_v is described by a solidifying Kelvin chain of ten units, the viscous flow, ϵ_f related to long term creep, is described by the aging dashpot, and additionally the hygral, ϵ_{sh} , and thermal, ϵ_T , strains are accounted for, dependent on the relative humidity and temperature evolution.

Using the strain additivity, the total strain rate can be expressed as the summation of the different strain rates, such that

$$\dot{\epsilon}_{tot} = \dot{\epsilon}^* + \dot{\epsilon}_v + \dot{\epsilon}_f + \dot{\epsilon}_{sh} + \dot{\epsilon}_T \quad (3)$$

with ϵ_{tot} the total strain, ϵ^* , the elastic strain given by the fraction of stress over instantaneous elastic modulus, $\epsilon^* = \frac{\sigma}{E_0}$, where $E_0 = \frac{1}{\xi_1}$, with ξ_1 a parameter related to the compliance of the elastic spring, the shrinkage strain rate is proportional to the rate of relative humidity, $d\epsilon_{sh} = k_{sh}dh$, where k_{sh} is the shrinkage coefficient, and the thermal strain rate is proportional to the temperature rate, $d\epsilon_T = \alpha_T dh$, where α_T is the coefficient of thermal expansion. The aging viscoelastic component is formulated as

$$\dot{\epsilon}_v(t) = \frac{\dot{\gamma}}{u(\alpha_c)} \quad (4)$$

where,

$$\gamma = \int_0^t \Phi(t_r(t) - t_r(\tau)) \mathbf{G} \dot{\sigma} d\tau \quad (5)$$

is the viscoelastic micro-strain of the cement gel, $u(\alpha_c) = (\alpha_c/\alpha_c^\infty)^{n_\alpha}$, is an aging function that expresses the volume fraction of cement gel produced by early-age chemical reactions, and depends on the total reaction degree, α_c , on the asymptotic reaction degree α_c^∞ , and on the material parameter n_α . In that case, a non-aging micro-compliance function of $\Phi(t - t') = \xi_2 \ln [1 + (t - t')^{0.1}]$ for the cement gel is assumed, with $t - t'$ the relative time after loading, and ξ_2 a parameter related to the viscoelastic response of the Kelvin chain, and the reduced time can be described as a result of changes in relative humidity and temperature, with

$$t_r(t) = \int_0^t \psi(\tau) d\tau \quad (6)$$

ψ represents the dependence of the micro-prestress relaxation on temperature and humidity as:

$$\psi(\tau) = [\alpha_s + (1 - \alpha_s) h^2] \exp\left(\frac{Q_s}{R} \left(\frac{1}{T_0} - \frac{1}{T}\right)\right) \quad (7)$$

where Q_s is the activation energy, R Boltzman's gas constant, T_0 room temperature in Kelvin, $\alpha_s = 0.1$, parameter, and $Q_s/R = 3000\text{K}$, [2]. The non-aging microcompliance function $\Phi(t - t')$, can be approximated, for numerical applications, using Dirichlet series [4, 5], yielding a rheological representation in the form of a Kelvin-chain.

For the last component of the rheological model, we can express the viscous flow as:

$$\dot{\epsilon}_f = \frac{\sigma}{\eta_f} \quad (8)$$

The dependence of the dashpot viscosity $\eta_f = 1/cS$ on time is captured through it's dependence on the microprestress S , which is the

stress due to changes in volume, during the hydration process; c = a constant of the Microstress theory. The rate of microstress is given by:

$$\dot{S} + \psi_s(T, h) c_0 \cdot S^2 = k_1 |dT \ln h + T dh/h| \quad (9)$$

3 Numerical Application

3.1 Calibration

In order to be able to quantify the effect of creep on fastening systems, for concrete class C25/30, it is essential to have both the mechanical and the HTC model well calibrated. In this investigation data from the extended creep and shrinkage database are used for the calibration of the concrete creep model. Particularly data from Brooks [7] of cylindrical specimens have been selected. The specimens with diameter $d = 76\text{mm}$ and length of $l = 255\text{mm}$, with water to cement ratio $w/c = 0.54 - 0.58$, cement content $c = 311 - 337 \text{ kg/m}^3$ and aggregate to cement ratio, $a/c = 4.75$, are loaded at $t' = 14\text{days}$ at 0.3 of their strength.

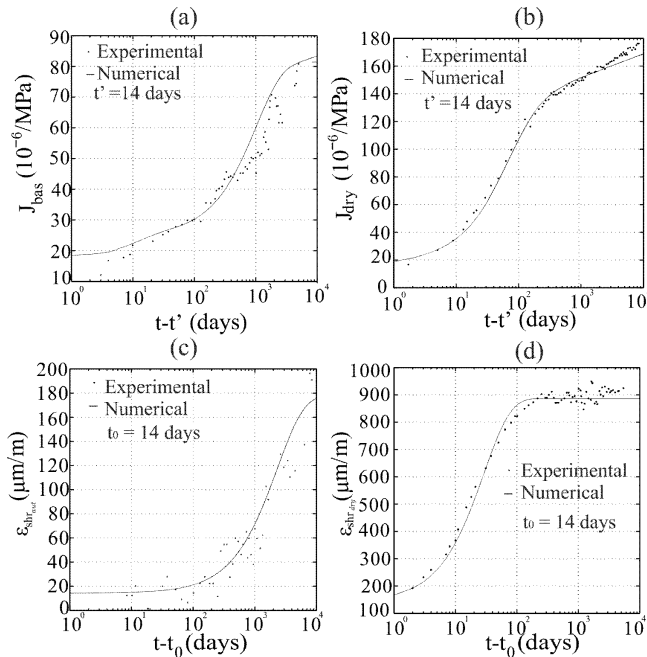


Figure 2: Creep compliances for (a) sealed, and (b) drying specimens respectively; autogenous and drying shrinkage strains are plotted in Figures (c) and (d)

The drying tests were performed in constant relative humidity of $h = 0.6$. In Figure 2 calibration and validation curves are shown for both

DOI 10.21012/FC9.141 autogenous and drying shrinkage, as well for basic and drying creep, while in Figure 3 the evolution of relative humidity in a cross section of the cylinders is presented.

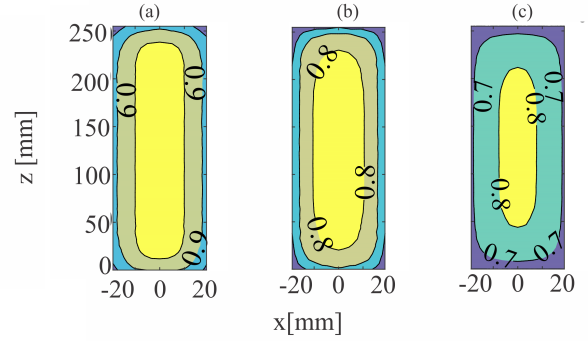


Figure 3: Relative humidity profiles at $t = 3, 25$ and 160days after exposing to environmental conditions

In Figure 3, an axis symmetrical gradient of relative humidity is shown. Furthermore, the drying process seems to continue after half a year, for a specimen of that dimensions, and geometry.

3.2 Application to Fastenings

The calibrated HTC model, creep and shrinkage models, are used to quantify numerically the effect of concrete creep on two different fastenings configurations, for a bonded anchor of epoxy based mortar. In particular, a bonded anchor, of diameter $d = 12\text{mm}$, is posted in a slab of concrete of $30 \cdot 30 \cdot 30\text{mm}$, with an embedment depth of $h_{eff} = 70\text{mm}$, and is loaded in tension at different ages, at 40% of the maximum load capacity. The concrete slab is supported by a steel ring with an inner diameter $d_{inn} = 22\text{mm}$ and an outer diameter of $d_{out} = 44\text{mm}$ in case of close support. Furthermore, in the other configuration, the same type of anchor is posted at the same depth, but in a larger slab of $50 \cdot 50 \cdot 30\text{cm}$ and a ring of $d_{inn} = 300\text{mm}$ and $d_{out} = 400\text{mm}$ is used. For both configurations the slabs start to dry at $t_0 = 3\text{days}$, at $h = 0.5$. In this contribution mortar is simulated using an interface law that follows an elastic bond law, calibrated using 4 pull-out tests as is shown in Figure 4.

In these various pull-out tests, anchors had the same characteristic as is aforementioned, but they were installed with an embedment depth of $h_{eff} = 65\text{mm}$.

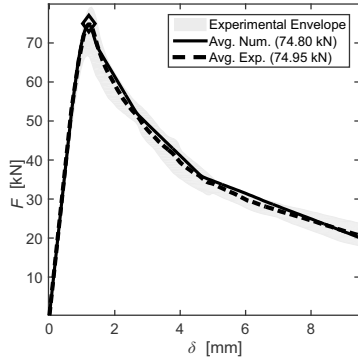


Figure 4: Calibration of elastic bond law

In Figure 5, the evolution of relative humidity, h and aging degree, λ , along the anchor is shown. It is obvious that the curing state is variable along the anchor and only after several months reaches an approximately uniform drying state while the maturity of concrete even after 5 years is still far from uniform.

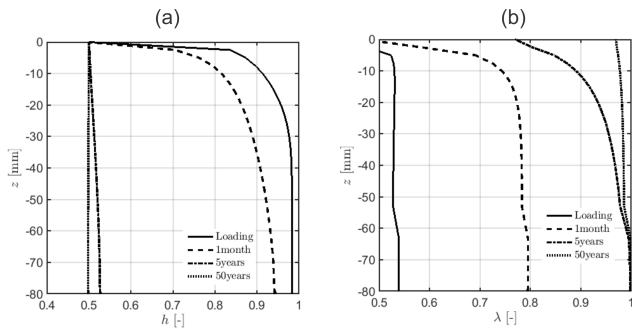


Figure 5: relative humidity (a) and aging degree (b) along the depth for 4 different ages

The response of the confined (close support) system in terms of deformation on the top of the anchor is shown in Figure 6. Figure 6(a) portrays the load deflection diagram of an anchor loaded at **7 and 150 days**. In agreement with the linearity limit in concrete design a relative sustained load level of 40% of the maximum capacity $F_{max} = 86\text{kN}$ was chosen. In Figure 6(b) the difference in creep deformations

DOI 10.21012/FC9.141 depending on the loading age are presented. As expected the system loaded at a younger age exhibits larger deformations. However, more importantly a given displacement limit is reached significantly faster.

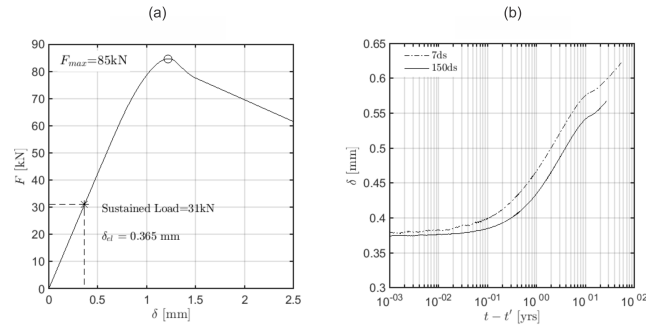


Figure 6: Response of pull out simulation (a) and the creep response (b) for a confined configuration

The design of fastening systems is generally based on the so called uniform bond law. While this approach is suitable for the design at the ultimate limit state, at service loads the distribution of bond stresses is far from uniform is presented in Figure 7, thick solid line. Over time, stresses are redistributed due to concrete creep causing a further deviation from the uniformity assumption of bond stress as well as a significant increase in stress by almost 50% after 50 years.

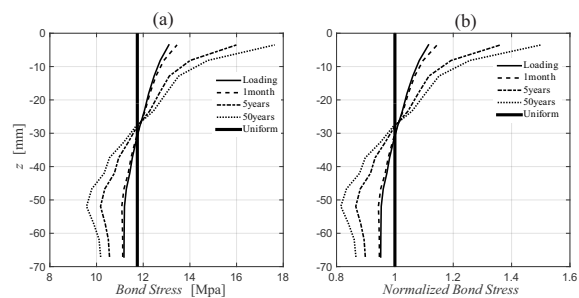


Figure 7: Bond stress (a) and bond stress normalized to uniform bond stress (b) for a confined configuration, for 4 different ages

Finally, the stress redistribution is not only caused by concrete creep but also by progressively growing damage as indicated in Figure 8, which shows the increasing maximum crack

opening with age in agreement with the evolution of the bond stress profiles of Figure 7.

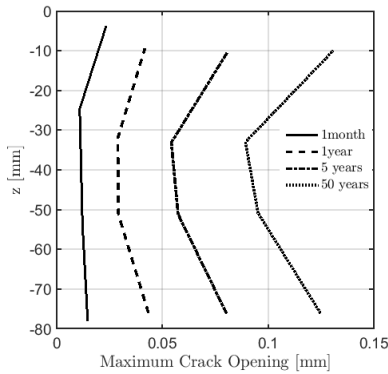


Figure 8: Maximum crack opening detected in different depths across the anchor

We repeat the simulations for the second configuration, using a larger ring to support concrete, and we acquire a response that is shown in Figure 9, as well as the evolution of the bond stress, which again is diverging from an assumed bond law, as is shown in Figure 10.

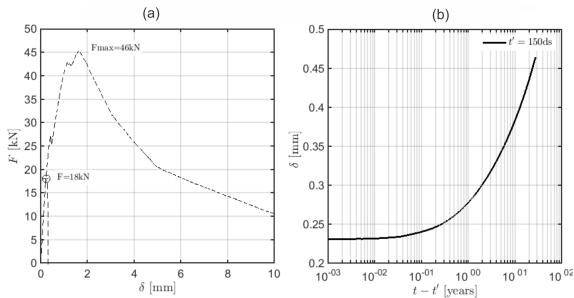


Figure 9: Response of pull out simulation (a) and creep response (b) for an unconfined configuration

Again a load of 40% of system’s ultimate capacity, $F_{max} = 46\text{kN}$ is chosen. In that case, the additional deformation in course of time, is significantly larger, if it is compared to the initial elastic deformation of $\delta_{el} = 0.23\text{mm}$, and reaches an increase of 100%, after 28years. The reason is that this configuration “activates” a larger amount of concrete, and consequently

DOI 10.21012/FC9.141 leads to higher concrete creep related deformations. Additionally, the deviation from a uniform bond law, is again high, reaching almost 70%, after 12 years.

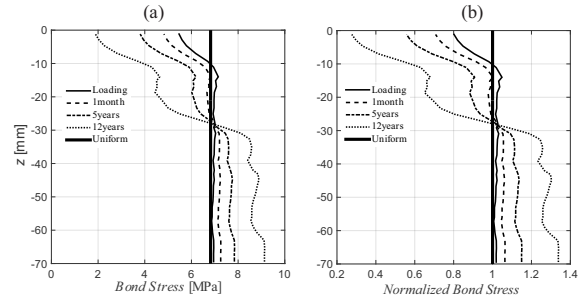


Figure 10: Bond stress (a) and normalized to uniform bond strength (b) for a confined configuration, for 4 different ages

4 CONCLUSIONS

In this contribution a numerical study of the concrete creep contribution to the long-term deformations of fastening systems is presented. By coupling models for the governing chemical and physical phenomena with the mechanical response a typical bonded anchor systems under sustained load was investigated. The simulated load was maintained for 50 and 14 years respectively. The preliminary numerical analysis of the system response, taking into account only concrete creep, shows:

- continuously increasing deformations even after 50 years for the confined case (with close support).
- only slightly higher relative deformations - δ_{cre}/δ_{el} - for the unconfined case
- significant divergence from a uniform bond law at service loads, especially at higher ages
- progressive damage in course of time

The presented numerical investigation shows strong indications that concrete creep is not negligible for the deformation prediction of bonded anchors. Further numerical studies, taking into account the viscoelastic nature of the

mortar layer, are required. In parallel, an experimental study of both described configurations is about the start at the time this paper is written, in order to provide better insights into the real system response, to refine the existing numerical models and extrapolation methods, and to be able to predict more accurately the long-term performance of bonded anchors which will ultimately ensure safer design.

REFERENCES

- [1] Alnaggar, M., Cusatis, G., and Di Luzio, G. (2013). “Lattice discrete particle modeling (LDPM) of alkali silica reaction (ASR) deterioration of concrete structures.” *Cement and Concrete Composites*, 41, 45–59.
- [2] Bažant, Z. P., Hauggaard, A. B., Baweja, S., and Ulm, F. (1997a). “Microprestress solidification theory for concrete creep. I: aging and drying effects.” *Journal of Engineering Mechanics*, 123 (11), 1188–1194.
- [3] Bažant, Z. P., Hauggaard, A. B., and Baweja, S. (1997b). “Microprestress solidification theory for concrete creep. II: Algorithm and verification.” *Journal of Engineering Mechanics*, 123 (11), 1195–1201.
- [4] Bažant, Z. P., and Prasannan, S. (1989a). “Solidification theory for concrete creep. I: formulation.” *Journal of Engineering Mechanics*, ASCE 115, 1691–1703.
- [5] Bažant, Z. P., and Prasannan, S. (1989a). “Solidification theory for concrete creep. II: verification and application.” *Journal of Engineering Mechanics*, ASCE 115, 1704–1725.
- [6] Brooks, J. J. (1984). DOI 10.21012/FC9.141 “Accuracy of estimating long term strains in concrete.” *Magazine of Concrete Research*, 36, 131–145.
- [7] Brooks, J. J. (1984). “Accuracy of estimating long term strains in concrete.” *Magazine of Concrete Research*, 36, 131–145.
- [8] Cusatis, G., Pelessone, D., and Mencarelli, A. (2011a). “Lattice Discrete Particle Model (LDPM) for failure behavior of concrete. I: Theory.” *Cement and Concrete Composites*, 33 (9), 881–890.
- [9] Cusatis, G., Mencarelli, A., G., Pelessone, D., and Baylot, J. (2011b). “Lattice Discrete Particle Model (LDPM) for failure behavior of concrete. II: Calibration and validation.” *Cement and Concrete Composites*, 33 (9), 891–905.
- [10] Di Luzio, G., and Cusatis, G. (2009b). “Hygro-thermo-chemical modeling of high performance concrete. II: Numerical implementation, calibration, and validation.” *Cement and Concrete Composites*, 31 (5), 309–324.
- [11] Di Luzio, G. (2009). “Numerical model for time-dependent fracturing of concrete.” *Journal of engineering mechanics*, 135 (7), 632–640.
- [12] Hubler, M. H., Wendner, R., and Bažant, Z. P. (2015a). “Comprehensive database for concrete creep and shrinkage: analysis and recommendations for testing and recording.” *ACI Materials Journal*.